Signatures of a Hidden Cosmic Microwave Background

Joerg Jaeckel,[1] Javier Redondo,[2] and Andreas Ringwald[2]

[1]*Institute for Particle Physics and Phenomenology, Durham University, Durham DH1 3LE, United Kingdom*
[2]*Deutsches Elektronen-Synchrotron DESY, Notkestraße 85, D-22607 Hamburg, Germany*

(Received 23 May 2008; published 26 September 2008)

If there is a light Abelian gauge boson γ' in the hidden sector its kinetic mixing with the photon can produce a hidden cosmic microwave background (HCMB). For meV masses, resonant oscillations $\gamma \leftrightarrow \gamma'$ happen after big bang nucleosynthesis (BBN) but before CMB decoupling, increasing the effective number of neutrinos $N_\nu^{\rm eff}$ and the baryon to photon ratio, and distorting the CMB blackbody spectrum. The agreement between BBN and CMB data provides new constraints. However, including Lyman-α data, $N_\nu^{\rm eff} > 3$ is preferred. It is tempting to attribute this effect to the HCMB. The interesting parameter range will be tested in upcoming laboratory experiments.

DOI: 10.1103/PhysRevLett.101.131801 PACS numbers: 98.80.Cq, 12.60.Cn, 14.70.Pw, 98.70.Vc

Most embeddings of the standard model into a more unified theory, in particular, the ones based on supergravity or superstrings, predict the existence of a hidden sector whose inhabitants have only very weak interactions with the standard model. The gauge interactions in the hidden sector generically involve $U(1)$ factors. Usually, it is assumed that the corresponding gauge bosons are very heavy. However, in realistic string compactifications, one of these hidden photons may indeed be light, with a mass in the sub-eV range, arising from a Higgs or Stückelberg mechanism. In this case, the dominant interaction with the visible sector photon will be through gauge kinetic mixing [1]; i.e., the system can be parametrized by the effective Lagrangian,

$$-\frac{1}{4}(F_{\mu\nu})^2 - \frac{1}{4}(B_{\mu\nu})^2 + \frac{\sin\chi}{2} B_{\mu\nu}F^{\mu\nu} + \frac{\cos^2\chi}{2} m_{\gamma'}^2 (B_\mu)^2,$$

where $F_{\mu\nu}$ and $B_{\mu\nu}$ are the photon (A^ν) and hidden photon (B^ν) field strengths. The dimensionless mixing parameter $\sin\chi$ can be generated at an arbitrarily high energy scale and does not suffer from any kind of mass suppression from the messenger particles communicating between the visible and the hidden sector. This makes it an extremely powerful probe of high scale physics. Predicted values for χ in realistic string compactifications range between 10^{-16} and 10^{-2} [2].

The most prominent implication of the kinetic mixing term is that, similar to neutrino mixing, the propagation and the interaction eigenstates are misaligned. The kinetic mixing can be removed by changing the basis $\{A, B\} \to \{A_R, S\}$, where $A_R = \cos\chi A$, $S = B - \sin\chi A$. Since A and A_R differ only by a typically unobservable charge renormalization we will drop the R subscript from now on. In the $\{A, S\}$ basis the kinetic term is diagonal but the kinetic mixing appears now as mass mixing in the mass term $(\sin\chi A_\mu + \cos\chi S_\mu)^2 m_{\gamma'}^2/2$. As a result one expects photon-sterile oscillations [3].

In this Letter, we examine the implications of this simple scenario for late cosmology. We focus on the meV mass range where a thermal population of hidden photons can be created through resonant oscillations after BBN but before CMB decoupling. This "hidden CMB" (HCMB) will contribute to the effective number of additional neutrinos at decoupling and, since some photons will disappear, will increase the baryon to photon ratio with respect to the BBN value. Moreover, we find that, in a certain parameter range, the blackbody spectrum of the CMB is distorted in a measurable way.

Effects of a post BBN HCMB production.—Let us assume that at the time of BBN there is no γ' thermal bath present. If kinetic mixing is the only interaction with standard model particles, this will be justified later. Additional particles charged under the hidden $U(1)_h$ appear as minicharged particles (MCPs) which could mediate the formation of an earlier HCMB. Given the existing constraints on MCPs [4] we will not discuss this possibility.

The oscillations $\gamma \leftrightarrow \gamma'$ decrease the photon number and energy density (n_γ, ρ_γ) leaving the total energy unchanged. The key parameter will be the fraction of ρ_γ that is converted into hidden photons, $x \equiv \rho_{\gamma'}/\rho_\gamma$.

We will see that inelastic processes are effective after HCMB decoupling. Therefore, the remaining photons will regain a black body distribution, albeit, due to the energy loss, at a lower temperature,

$$T_{\rm after} = (1-x)^{1/4} T_{\rm before}. \tag{1}$$

Since neutrinos remain unchanged during the HCMB formation, the ratio of neutrino and photon temperatures will also increase. The invisible energy density (in radiation) at decoupling can be estimated using CMB anisotropies and is often quoted as the effective number of "standard" neutrinos, by normalizing it with $\rho_\nu = (7/8)(4/11)^{4/3}\rho_\gamma$. In our case,

$$N_\nu^{\rm eff} \equiv \frac{\rho^{\rm total} - \rho_\gamma}{\rho_\nu} = \frac{N_\nu^{\rm std}}{(1-x)} + \frac{x}{1-x}\frac{8}{7}\left(\frac{11}{4}\right)^{4/3} \tag{2}$$

is the sum of neutrino and hidden photon contributions.

Strong limits on $N_\nu^{\rm eff}$ at decoupling arise from global fits of CMB anisotropies alone [5] or combined with large scale structure data [6]. Inclusion of Lyman-α data favors values $N_\nu^{\rm eff} > 3$ [7], although this might well be due to systematics [8]. A recent analysis of WMAP5 plus other CMB anisotropy probes, large scale structure (no Ly-α) and supernovae data provides [9]

$$N_\nu^{\rm eff} = 2.9^{+2.0}_{-1.4} \quad (95\%\ \text{C.L.}), \tag{3}$$

which, using the standard, $N_\nu^{\rm std} = 3.046$, turns (3) into

$$x \lesssim 0.20. \tag{4}$$

As an illustration of the inclusion of Ly-α data we can take $N_\nu^{\rm eff} = 3.8^{+2.0}_{-1.6}(95\%\ \text{C.L.})$ [8], whose central value gives $x \simeq 0.1$ (values as high as $N_\nu^{\rm eff} = 5.3$ can be found in the literature [7], so choosing $N_\nu^{\rm eff} = 3.8$ from [8] seems relatively conservative). The Planck satellite data [10] could be used to reach a sensitivity down to $\Delta N_{\rm eff} = 0.07$, corresponding to $x \sim 0.01$.

Since n_γ is proportional to T^3, the baryon to photon ratio (which would otherwise remain constant) is also modified according to

$$\eta^{\rm after} = (1 - x)^{-(3/4)}\eta^{\rm before}. \tag{5}$$

Indeed the value for η inferred from the abundances of the light elements produced at BBN and the one obtained by measuring temperature fluctuations in the CMB [9] agree within their error bars,

$$\eta^{\rm BBN} = 5.7^{+0.8}_{-0.9} \times 10^{-10} \quad (95\%\ \text{C.L.}), \tag{6}$$

$$\eta^{\rm CMB} = 6.14^{+0.3}_{-0.25} \times 10^{-10} \quad (95\%\ \text{C.L.}), \tag{7}$$

which allows us to set the bound $x \lesssim 0.32$.

Photon oscillations in the early universe plasma.—The formalism to study the dynamics of a thermal bath of particles that undergo "flavor" oscillations among the different species was developed some time ago [11,12], for a textbook treatment see [13]. The state of an ensemble of γ and γ' is described by a 2-by-2 density matrix,

$$\rho = (1 + \mathbf{P}\cdot\boldsymbol{\sigma})/2, \tag{8}$$

where $\boldsymbol{\sigma}$ has the Pauli matrices as components and $\mathbf{P}$ is a "flavor polarization vector" carrying all the information of the ensemble. Its modulus gives the degree of coherence, $P_z = 1$ (-1) corresponding to a pure γ (γ') state, while $|\mathbf{P}| = 0$ to a completely incoherent state, which of course defines the state of "flavor equilibrium." The transverse components $P_{x,y}$ contain the quantum correlations.

The time evolution of the ensemble is given by a precession of $\mathbf{P}$ (flavor oscillations) and a shrinking of its transverse component (decoherence due to absorption and scattering), according to Stodolsky's formula [12]

$$\dot{\mathbf{P}} = \mathbf{V}\times\mathbf{P} - D\mathbf{P}_T. \tag{9}$$

Here $\mathbf{V}$ is the "flavor magnetic field" given by

$$\Delta\begin{pmatrix}\sin2\chi_{\rm eff}\\ 0\\ \cos2\chi_{\rm eff}\end{pmatrix} \equiv \frac{m_{\gamma'}^2}{2\omega}\begin{pmatrix}\sin2\chi\\ 0\\ \cos2\chi\end{pmatrix} - \frac{\omega_P^2}{2\omega}\begin{pmatrix}0\\ 0\\ 1\end{pmatrix}, \tag{10}$$

where ω is the γ, γ' energy and we have included the refraction properties of the medium (basically an electron plasma) as a photon "effective mass", given by the plasma frequency $\omega_P^2 \simeq 4\pi\alpha n_e/m_e$ with α the fine-structure constant, and m_e, n_e the electron mass and density. The damping factor D equals half the collision rate of photons [12], here dominated by Thomson scattering, $\Gamma_C \simeq 8\pi\alpha^2/(3m_e^2)n_e$.

Before dealing with the details of the calculation, we will try to gain some intuition about the main points of the cosmology of the $\gamma - \gamma'$ system. For temperatures below $0.04m_e \sim 20$ keV, electrons and positrons have annihilated leaving an electron relic density which balances the charge of protons, namely $n_e \simeq n_B = \eta n_\gamma = \eta 2\zeta(3)T^3/\pi^2$. Using the BBN central value (6), we find

$$\omega_P^2 \simeq (0.16\ \text{meV})^2\,(\text{T/keV})^3. \tag{11}$$

As the universe expands, the density decreases and so do the plasma mass and absorption rate. The ratio $R \equiv \omega\Gamma_C/\omega_P^2$ is, however, independent of n_e and very small, $2\alpha\omega/(3m_e) \sim 10^{-5}$ (ω/keV). Therefore the damping term D in (9) is typically smaller than the precession rate Δ, the only possible exception being the resonant case to be discussed later. In this situation we can use the precession-averaged $\mathbf{P}_T$ in (9), which then turns into $\langle|\dot{\mathbf{P}}|/|\mathbf{P}|\rangle = -\cos^2 2\chi_{\rm eff}\sin^2 2\chi_{\rm eff}\Gamma_C/2 \equiv \tilde{\Gamma}$ [13]. Under these conditions a significant HCMB will form if the rate $\tilde{\Gamma}$ exceeds the expansion rate of the universe, given by the Hubble parameter $H = 2.5 \times 10^{-22}$ $(\text{T/keV})^2$ eV.

Isocontours of $\tilde{\Gamma}/H = 1$ are plotted in Fig. 1, showing the possible history of the HCMB formation for different values of $m_{\gamma'}$ and $\sin\chi$. During its evolution, the universe moves on a horizontal line of fixed χ from high T (right) to

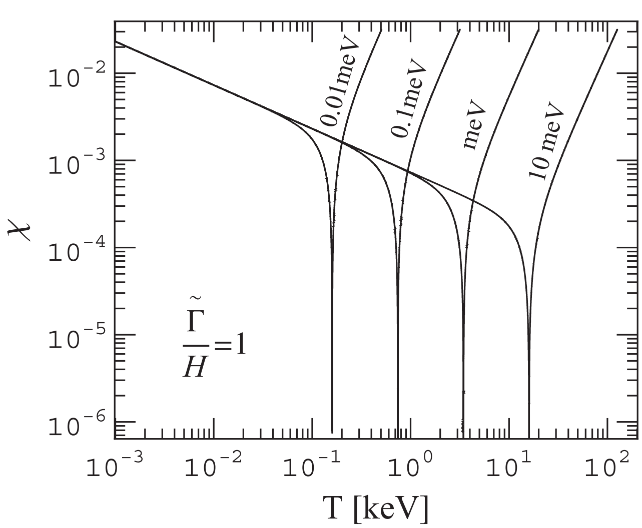

FIG. 1. Isocontours of $\tilde{\Gamma}/H = 1$ for different γ' masses.

low T (left). We can clearly distinguish three different regimes separated in time by a resonant peak occurring at $T^{\rm res}$, the temperature at which ω_P^2 has decreased enough to match exactly $m_{\gamma'}^2 \cos 2\chi$.

(i) In an early stage, for $T \gg T^{\rm res}$, ω_P is much larger than $m_{\gamma'}$; photons are very close to being both interaction and propagation eigenstates and $\gamma - \gamma'$ oscillations are strongly suppressed by the effective mixing angle given by

$$\sin 2\chi_{\rm eff} \simeq \frac{m_{\gamma'}^2}{\omega_P^2} \sin 2\chi \ll \sin 2\chi. \qquad (12)$$

This is in contrast to the usual cosmology of exotic particles. Light hidden photons are completely decoupled for high enough temperatures (as long as their only relevant coupling is the kinetic mixing). This justifies our earlier claim and allows us to set the initial conditions for the $\gamma - \gamma'$ system to $P_z = +1$, i.e., a pure photon bath. As the temperature approaches $T^{\rm res}$, $\sin 2\chi_{\rm eff}$ becomes larger than $\sin 2\chi$. Production of γ' is effective when crossing the $\tilde{\Gamma}/H = 1$ line in Fig. 1.

(ii) In a small region around $T^{\rm res}$, the production can be effective even for very small χ. However, the precession average is not justified because typically $\Delta^{\rm res} \ll D$. Below we provide details on the calculation in this regime.

(iii) For $T \ll T^{\rm res}$, the averaging procedure is again justified. In this regime, $m_{\gamma'} \gg \omega_P$ and we recover the well known vacuum case. The evolution will again freeze out after crossing the $\tilde{\Gamma}/H = 1$ line in Fig. 1.

Resonant production.—From Fig. 1 it is clear that for $\chi \lesssim 6 \times 10^{-6}$ (larger values are excluded; see Fig. 2) production is effective only in the resonant regime. Therefore, we need an approximation that is valid in the vicinity of the resonance. Moreover, since the resonance happens only for a short period of time, the simple criterion $\tilde{\Gamma}/H > 1$ is not sufficient to ensure that a sizable HCMB is produced so we have to calculate the integrated production.

In the vicinity of the resonance, the oscillation frequency is minimal ($\Delta^{\rm res} \equiv m_{\gamma'}^2 \sin 2\chi/(2\omega)$) and indeed typically much smaller than the damping factor Γ_C. The flavor relaxation rate, in a general "strong damping" regime, is given by [12]

$$\bar{\Gamma} = V_T^2 \frac{D}{D^2 + V_z} = \frac{1}{2} \frac{\sin^2 2\chi}{r^2 + (\cos 2\chi - y)^2} \Gamma_C, \qquad (13)$$

with $y \equiv \omega_P^2/m_{\gamma'}^2$ and $r \equiv \omega \Gamma_C/m_{\gamma'}^2$. The strong damping condition reads simply $r \gg \sin 2\chi$. In the interesting region $\chi \lesssim 6 \times 10^{-6}$ this is typically fulfilled because $r \simeq R \simeq 10^{-5}$ (ω/keV). At the low-energy end of the spectrum we will violate the strong damping regime, but this region contributes little to the energy density.

The physical meaning of (13) is clear regarding (9). Since D damps $\mathbf{P}_T$, $\mathbf{P}$ will rapidly become attached to the z axis. Note that, for $|\mathbf{V}_T| \equiv \Delta \sin 2\chi_{\rm eff} = 0$, $\mathbf{P}_T = 0$ is a *stationary* solution of (9) for which the production rate would vanish. Now let us switch on a small $\mathbf{V}_T \neq 0$. The

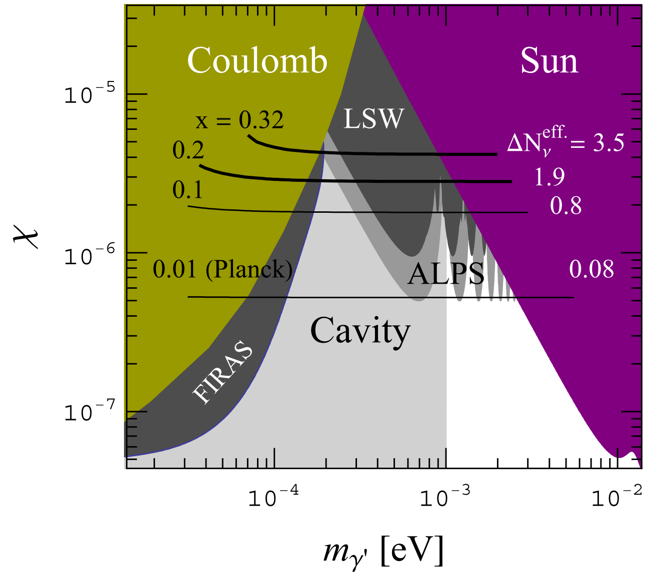

FIG. 2 (color online). Isocontours of $x \equiv \rho_{\gamma'}/\rho_\gamma$ at the CMB epoch in the mass-mixing plane. The region above $x = 0.32$ is excluded by the agreement between the baryon to photon ratio inferred from BBN and CMB data, while $x > 0.2$ is excluded by the upper limits on the effective number of neutrinos $N_\nu^{\rm eff} = 3.046 + \Delta N_\nu^{\rm eff}$ at the CMB epoch. Future Planck data [10] could push the bound to $x \simeq 0.01$. Distortions of the CMB blackbody would be unacceptable in the region FIRAS. Also shown are the bounds from Coulomb law tests [22], CAST (Sun) [23], and light-shining-through-walls (LSW) experiments (current [17] and near future "ALPS" [18]). The region labeled "Cavity" can be explored with microwave cavities [20] and the remaining region at higher masses with further solar γ' searches [24].

precession caused by $\mathbf{V}_T$ tries to move $\mathbf{P}$ away from the z axis. However, any transverse component is immediately damped away again because $D \gg |\mathbf{V}_T|$. While the precession keeps $|\mathbf{P}|$ constant, it is decreased by the damping and flavor equilibrium is approached at a rate (13).

Integrating Eqs. (9) and (13) over time we can calculate the $\gamma \leftrightarrow \gamma'$ transition probability,

$$P_{\gamma \to \gamma'}(T_f) = \frac{1}{2}\left(1 - \exp\left\{\int_\infty^{T_f} \frac{\bar{\Gamma}}{H} \frac{dT}{T}\right\}\right), \qquad (14)$$

where we have used a parametrization in terms of the temperature T instead of time. Since the relevant part of the integral comes from the vicinity of the resonance, we expand the denominator of $\bar{\Gamma}$ around $y = 1$ up to the relevant quadratic term. In terms of $z = \sqrt[3]{y}$, $w = \omega/T^{\rm res}$, and approximating $\sin 2\chi \simeq 2\chi$, the integral is,

$$\frac{1}{2}\int \frac{\bar{\Gamma}}{HT} dT \simeq \chi^2 \left[\frac{\Gamma_C}{HT}\right]^{\rm res} \int \frac{T^{\rm res} dz}{R^2 + 9(z-1)^2} \simeq \chi^2 \left[\frac{\Gamma_C}{H}\right]^{\rm res} \frac{\pi}{3R}$$
$$= \frac{\pi}{3} \frac{m_{\gamma'}^2 \chi^2}{H^{\rm res} \omega} = \frac{1.0 \times 10^{11} \chi^2}{w},$$

where we have evaluated the braced combination at $T^{\rm res}$.

Our main result, namely, the fraction of the energy stored in the HCMB, is obtained by integrating the probability over the Boltzmann distribution,

$$x = \frac{15}{\pi^4} \int_{w_0}^{\infty} \frac{w^3}{e^w - 1} P_{\gamma \to \gamma'} dw. \tag{15}$$

To be conservative we cut off the integral at small ω, where the strong damping approximation breaks down, $R \simeq 2\chi$, corresponding to $\omega_0 \simeq 2 \times 10^5 \chi$ keV. If χ is large, this can affect a sizable part of the spectrum. Otherwise, we obtain an analytic expression by expanding (14),

$$x \simeq 3.9 \times 10^{10} \chi^2. \tag{16}$$

The depletion of photons distorts the blackbody spectrum, measured by FIRAS to 10^{-4} accuracy [14]. However, double Compton scattering $\gamma e \to \gamma\gamma e$ erases any deviations from a blackbody present before $T \simeq 1.2$ keV [15], corresponding to $m_{\gamma'} > 0.2$ meV. The FIRAS bound resulting from a numerical calculation of the evolution of the distortions [15] is shown in Fig. 2.

Discussion and conclusions.—In the region $0.1 \text{ meV} \lesssim m_{\gamma'} \lesssim 10$ meV, the fraction of photons converted into hidden photons depends only very weakly on the mass [cf. Eq. (16) and Fig. 2]. For $\chi \gtrsim 10^{-5}$, the resonant production would be sufficiently strong to convert roughly half the photon energy into hidden photons. This would clearly be in contradiction with cosmological observations: even the conversion of a small part of the photon energy into hidden photons may leave observable traces in the effective number of relativistic species $N_\nu^{\rm eff}$ and in the baryon to photon ratio η. Using $x < 0.2$, from the upper limit on $N_\nu^{\rm eff}$ in (3), or the slightly weaker constraint $x \lesssim 0.32$, from the upper limit on η in (7), one obtains an upper bound $\chi \lesssim (3 - 4) \times 10^{-6}$, in the mass range $0.1 \text{ meV} \lesssim m_{\gamma'} \lesssim 10$ meV (cf. Fig. 2). In the mass range $0.15 \text{ meV} \lesssim m_{\gamma'} \lesssim 0.3$ meV, this improves upon the previously established upper bounds on χ—from searches for deviations from the Coulomb law and from light-shining-through-walls (LSW) experiments.

As mentioned earlier, inclusion of Lyman-α data seems to favor higher values of $N_\nu^{\rm eff} > 3$ [7,8]. It is certainly very speculative to suggest a hidden CMB on this basis alone (for an alternative interpretation see [16]), but the Planck satellite could eventually confirm (or rule out) such an excess in $N_\nu^{\rm eff}$. Fortunately, the interesting parameter region can be explored in the near future by pure laboratory experiments, notably by LSW experiments [17–19] or an experiment exploiting microwave cavities [20] (cf. Fig. 2), allowing an independent test of the HCMB hypotesis. Furthermore, the hidden photon CMB itself could be tested directly by an experiment like ADMX [21] in which hidden photons entering a cavity can be reconverted into detectable ordinary photons.

[1] B. Holdom, Phys. Lett. B **166**, 196 (1986); R. Foot and X. G. He, Phys. Lett. B **267**, 509 (1991).
[2] K. R. Dienes *et al.*, Nucl. Phys. **B492**, 104 (1997); S. A. Abel and B. W. Schofield, Nucl. Phys. **B685**, 150 (2004); S. A. Abel *et al.*, Phys. Lett. B **666**, 66 (2008); arXiv:0803.1449.
[3] L. B. Okun, Sov. Phys. JETP **56**, 502 (1982).
[4] S. Davidson, S. Hannestad, and G. Raffelt, J. High Energy Phys. 05 (2000) 003.
[5] K. Ichikawa *et al.*, arXiv:0803.0889; J. Dunkley *et al.* (WMAP Collaboration), arXiv:0803.0586.
[6] G. Mangano *et al.*, J. Cosmol. Astropart. Phys. 03 (2007) 006; K. Ichikawa, M. Kawasaki, and F. Takahashi, J. Cosmol. Astropart. Phys. 05 (2007) 007; E. Komatsu *et al.* (WMAP Collaboration), arXiv:0803.0547.
[7] U. Seljak *et al.*, J. Cosmol. Astropart. Phys. 10 (2006) 014; M. Cirelli and A. Strumia, J. Cosmol. Astropart. Phys. 12 (2006) 013.
[8] J. Hamann *et al.*, J. Cosmol. Astropart. Phys. 08 (2007) 021.
[9] V. Simha and G. Steigman, J. Cosmol. Astropart. Phys. 06 (2008) 016.
[10] Planck Collaboration, arXiv:astro-ph/0604069; L. Perotto *et al.*, J. Cosmol. Astropart. Phys. 10 (2006) 013; J. Hamann *et al.*, J. Cosmol. Astropart. Phys. 03 (2008) 004.
[11] R. A. Harris and L. Stodolsky, Phys. Lett. B **116**, 464 (1982).
[12] L. Stodolsky, Phys. Rev. D **36**, 2273 (1987).
[13] G. G. Raffelt, *Stars As Laboratories For Fundamental Physics* (University of Chicago Press, Chicago, USA, 1996), p. 664.
[14] D. J. Fixsen *et al.*, Astrophys. J. **473**, 576 (1996).
[15] L. Danese and G. De Zotti, Astron. Astrophys. **107**, 39 (1982).
[16] K. Ichikawa *et al.*, J. Cosmol. Astropart. Phys. 05 (2007) 008.
[17] M. Ahlers *et al.*, Phys. Rev. D **77**, 095001 (2008), and references therein.
[18] See http://alps.desy.de/e55; K. Ehret *et al.* (ALPS Collaboration), arXiv:hep-ex/0702023.
[19] C. Robilliard *et al.* (BMV Collaboration), Phys. Rev. Lett. **99**, 190403 (2007); A. S. Chou *et al.* (GammeV (T-969) Collaboration), Phys. Rev. Lett. **100**, 080402 (2008); A. Afanasev *et al.* (LIPSS Collaboration), arXiv:0806.2631 [Phys. Rev. Lett. (to be published)]; P. Pugnat *et al.* (OSQAR Collaboration), Report No. CERN-SPSC-2006-035; see http://graybook.cern.ch/programmes/experiments/OSQAR.html; G. Cantatore (PVLAS Collaboration), *3rd Joint ILIAS-CERN-DESY Axion-WIMPs Training Workshop, 2007* (University of Patras, Greece); more information can be found at http://axion-wimp.desy.de.
[20] J. Jaeckel and A. Ringwald, Phys. Lett. B **659**, 509 (2008); P. L. Slocum, *4th Patras Workshop on Axions, WIMPs and WISPs 2008, Hamburg*, http://axion-wimp.desy.de/e30.
[21] S. Asztalos *et al.*, Phys. Rev. D **64**, 092003 (2001).
[22] D. F. Bartlett and S. Logl, Phys. Rev. Lett. **61**, 2285 (1988); E. R. Williams, J. E. Faller, and H. A. Hill, Phys. Rev. Lett. **26**, 721 (1971).
[23] J. Redondo, J. Cosmol. Astropart. Phys. 07 (2008) 008.
[24] S. N. Gninenko and J. Redondo, Phys. Lett. B **664**, 180 (2008).